# A Map of Geothermal Potential for the Great Basin, USA: Recognition of Multiple Geothermal Environments

**Mark Coolbaugh[1], Richard Zehner[1], Corné Kreemer[2], David Blackwell[3], and Gary Oppliger[4]**

**[1]Great Basin Center for Geothermal Energy at University of Nevada, Reno (UNR)**
**[2]Nevada Geodetic Laboratory at Nevada Bureau of Mines and Geology (NBMG)**
**[3]Southern Methodist University (SMU) Geothermal Laboratory**
**[4]Arthur Brant Laboratory for Exploration Geophysics (ABLE Lab), UNR**

***Keywords***

*Geothermal, GIS, potential, favorability, Great Basin, map*

## ABSTRACT

A 1:1,000,000 scale geothermal favorability map of the Great Basin is currently being published through the Nevada Bureau of Mines and Geology (NBMG) and is now available at the web site (http://www.unr.edu/geothermal/geothermal_gis2.htm) of the Great Basin Center for Geothermal Energy (GBCGE). This map allows for separate assessment of the potential for magmatically heated and extensional-type geothermal systems. Added to the map are temperature gradient wells from the Southern Methodist Laboratory (SMU) and United States Geological Survey (USGS) databases, thermal springs and wells from the Geo-Heat Center-compiled geochemical database, and Quaternary faults from the USGS Quaternary Fault and Fold Database. A background 200-meter-resolution shaded digital topographic map provides reference for location.

Logistic regression was used to calculate a scaled favorability index on the map for extensional-type geothermal systems based on data input from maps of 1) horizontal gravity gradient, 2) horizontal topographic gradient, 3) crustal dilation as measured by GPS stations, 4) crustal extension calculated from slip rates along Quaternary faults, 5) temperature gradient in the upper crust, and 6) the number, magnitude, and distance to historic earthquakes. These input "evidence" maps were chosen in part for their ability to model geothermal potential independently of groundwater characteristics and lithologic permeabilities that influence the ability of hot springs or fumaroles to form. Coefficients for the favorability index were calculated outside of known regional aquifers and then used to predict favorability in the aquifer areas to assess the extent to which regional aquifers may be concealing geothermal activity. The results indicate that known geothermal systems ≥ 150° C are underrepresented in areas underlain by regional aquifers, in essence confirming that these regions are either concealing geothermal systems or are under-explored relative to their non-aquifer counterparts.

The factors controlling the location of extensional geothermal systems appear to change somewhat across the Great Basin. In the westernmost Great Basin (Walker Lane), geothermal systems are associated with higher earthquakes frequencies than in regions to the east, where steep gravity and topographic gradients are more diagnostic. These differences likely reflect a change in the character of active crustal tectonics across the basin, from relatively strike-slip dominant in the west, where pull-apart basins exist, to more purely extensional in the central and eastern portions in the basin.

## Introduction

A new geothermal potential map is being published through the NBMG (Coolbaugh et al., 2005) that is designed to serve as a regional guide for geothermal exploration geologists. The objective of the map is to identify areas in the Great Basin that are most likely to host high-temperature (> 150° C) geothermal systems capable of producing electrical energy. Three different maps have been overlaid to produce the overall map product shown in Plate 1 at the end of this paper. These 3 component maps are:

1) A favorability map for high-temperature (≥ 150°C) extensional-type geothermal systems. As defined by Koenig and McNitt (1983) and Wisian et al. (1999), extensional-type geothermal systems are those that do not obtain their heat from upper crustal magmas or cooling intrusions and instead are believed to owe their existence to active extensional tectonics (and Quaternary faults) and high regional heat flow. The background colors, superimposed on shaded topography, provide a ranking of the favorability for extensional-type geothermal systems.

2) A favorability map for high-temperature (≥ 150°C) magmatically heated geothermal systems. The favorability of *magmatically heated* geothermal systems is *not* specifically ranked by color here, but can be assessed qualitatively based

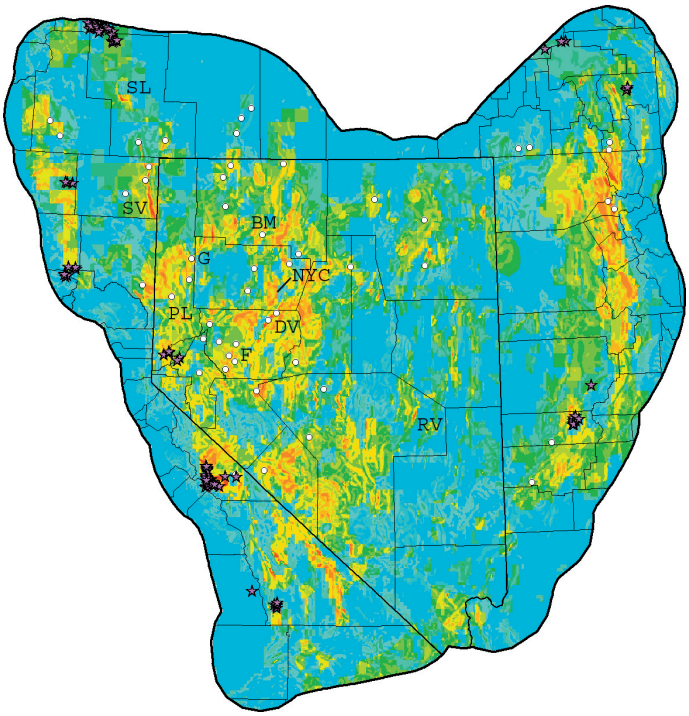


**Figure 1.** Favorability index for extensional geothermal systems in the Great Basin. Warmer colors indicate higher favorability. BM = Blue Mountain; DV = Dixie Valley; F = Fallon; G = Gerlach; NYC = New York Canyon; PL = Pyramid Lake; RV = Railroad Valley; SL = Summer Lake; SV = Surprise Valley. Circles are geothermal systems ≥ 150° C used as training points in the model. Stars are silicic volcanic vents ≤ 1.5 Ma.

on the occurrence of Quaternary silicic volcanic vents (see red stars, Plate 1; Figure 1. overleaf).

3) A geothermal information map. Superimposed on the scaled geothermal ranking for extensional systems are temperature gradient and heat flux measurements from wells (Southern Methodist University database), Quaternary faults (USGS compiled database), thermal springs and wells with geothermometer temperature estimates (Geo-Heat Center compiled database; Boyd, 2002), geothermal power plants, and known geothermal resource areas (KGRAs).

## Favorability Ranking—Extensional Geothermal Systems

Digital technology and evolving spatial statistical analytical techniques were availed of in order to produce an overall favorability map for extensional-type geothermal systems based on the integration of geothermal information contained in multiple maps that in the past were not available in computer digital format. The background colors on Plate 1 and Figure 1 represent a scaled geothermal favorability index: the higher the index value, the warmer the color. This classification is relative to the Great Basin only. Because the Great Basin has a relatively high geothermal favorability compared to most other areas of the United States (Blackwell and Richards, 2004), areas of low ranking on the Great Basin map might be considered favorable in the context of the entire continental United States, and could be favorable for lower-temperature (< 150°C) geothermal applications. The number of colors displayed on the map has been maximized in order to highlight local changes in favorability. The value of the geothermal index is statistically derived using several input "evidence" maps, which include maps of the horizontal gravity gradient, the horizontal topographic gradient, crustal dilation as measured by GPS stations, extension calculated from slip rates along Quaternary faults, the temperature gradient in the upper crust, and a map of the number, magnitude, and distance to historic earthquakes.

Fifty-one (51) geothermal systems in the Great Basin, those that are either producing electrical power today or have geothermometer temperatures ≥ 150°C, were used as "training sites" to assess the degree of correlation between the input evidence maps and geothermal activity. Weights-of-evidence statistical analysis was used to convert each real-number-based digital evidence map into a statistically significant number of ranked classes, based on the observed association with the geothermal systems. The gravity/topographic gradient evidence map was converted into 5 statistically significant classes of increasing gradient, while the crustal dilation and the temperature gradient evidence maps were each converted into maps with 3 levels of classification, and the earthquake evidence map was converted into a binary class map (favorable vs. unfavorable levels of earthquake occurrence). Logistic-regression was then used to combine the individual input evidence maps into a favorability index, and the color ranking on the map is proportional to the log-transformed logistic-regression posterior probability. Coolbaugh (2003) and Coolbaugh et al. (2002) provide more details on the application of weights of evidence and logistic-regression analysis for modeling geothermal favorability.

The borders of this geothermal map were defined by placing a 70 km buffer around the Great Basin boundary defined by Thelin and Pike (1991). By expanding the map to include this buffer, it becomes possible to display information on the margins of the Great Basin, where many geothermal systems, particularly the magmatically heated systems, occur.

Six geological/geophysical maps were combined into four evidence layers and used to model geothermal favorability. Each of these maps represents a new digital compilation not previously available or published until this year. A description of each of these four layers follows:

**Combined Gravity/Topographic Gradient Map (Figure 2A):** As a proxy for measuring the effective vertical displacement along late Tertiary and Quaternary faults in the Great Basin, a residual gravity map was combined with a topographic digital elevation model (DEM), and then the total surface slope (horizontal gradient) was calculated. The residual gravity map (a 20-km upward continued residual isostatic gravity anomaly) was further reduced by removing bedrock-only regional gravity trends to produce a basins-only gravity anomaly map. This gravity map was converted to an approximate equivalent amount of subsurface basement relief using 60 meters/mgal (equivalent to a density contrast of 0.4 g/cm$^3$), and then added to the 1-km DEM. The combined bedrock surface slope was then calculated by computing the total horizontal gradient for each 1-km cell.

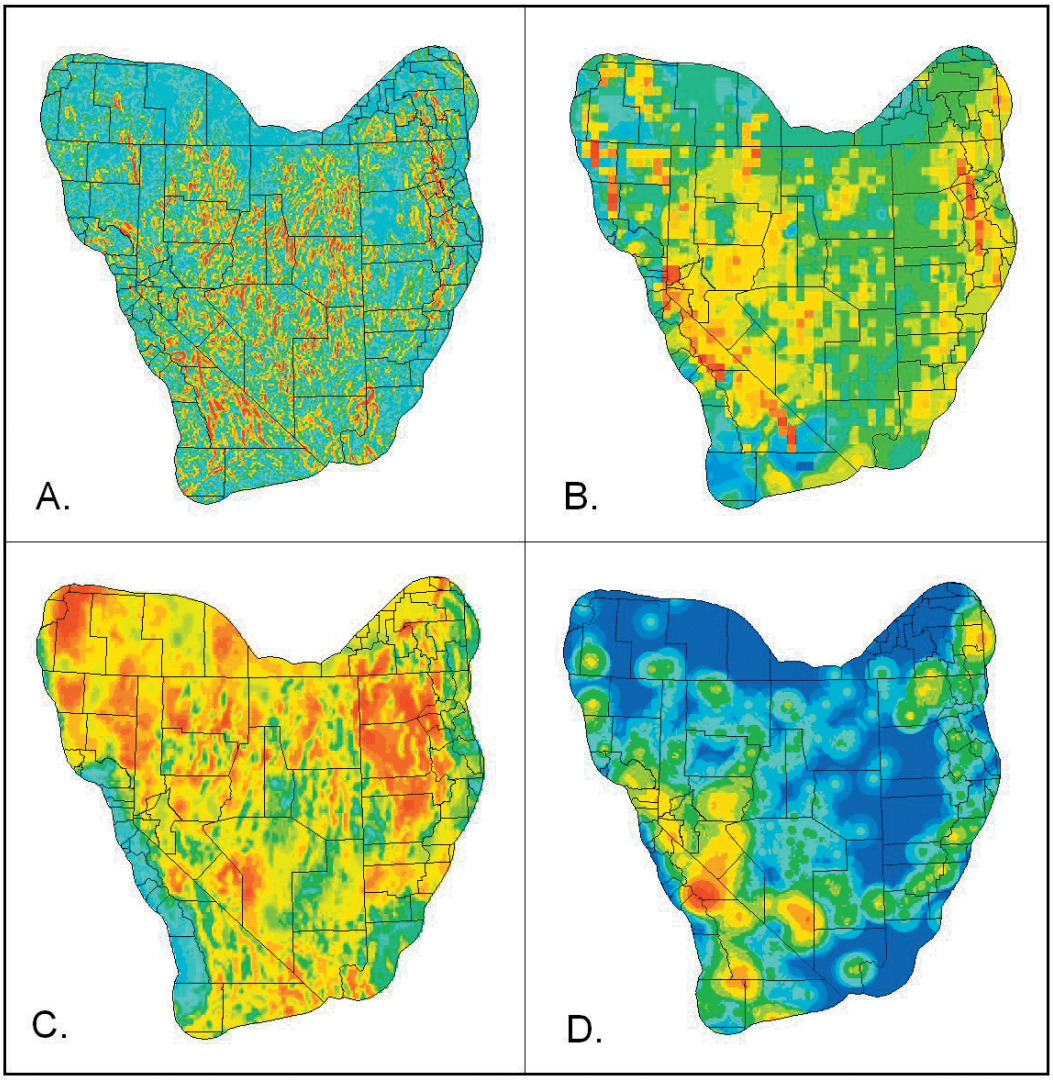


**Figure 2.** Input evidence maps used for calculating logistic regression favorability index for extensional geothermal systems: A) combined gravity and topographic gradient map (warmer colors have higher gradients); B) crustal dilation as estimated from GPS station velocity measurements and slip rates along Quaternary faults (warmer colors have greater rates of dilation); C) temperature gradient in the first kilometer of the crust (warmer colors have higher temperature gradients); and D) weighted sum of earthquake magnitudes (warmer colors have higher sums).

**Combined Global Positioning System (GPS) and Fault Dilation Map (Figure 2B):** Crustal dilation rates derived from GPS velocity measurements (interseismic strain) were averaged with dilation rates calculated from Quaternary fault slip rate data (long-term seismic strain) to produce a more geographically complete map of crustal dilation in the Great Basin. The geodetic strain rates were based on 476 GPS velocity measurements from stations located throughout and just outside the Great Basin. These velocities were compiled from multiple networks, including BARGEN, USGS campaigns, and other groups. Velocities affected by known magmatic/volcanic activity were excluded. A USGS Quaternary Fault and Fold Database (QFFD) (Machette, et al., 2003; http://qfaults.cr.usgs.gov/), was updated with slip rate estimates compiled in 1996 and 2002 (http://eqhazmaps.usgs.gov/html/faults2002.html). Slip rate parameters were converted to long-term strain rate tensors, from which dilation was calculated for every 20 km square grid cell in the Great Basin. The methodology used to obtain strain rate models from GPS velocities and fault parameters, presented and reviewed by Haines and Holt (1993), Holt et al. (2000) and Kreemer et al. (2000), is a rapidly evolving science. Significant improvements are expected in the future as the GPS station network expands and measurement accuracies improve. Future work should help resolve apparent disparities between short-term and long-term fault slip rates and clarify the distribution of slip along multiple sub-parallel fault segments.

**Temperature Gradient Map (Figure 2C):** A shallow crustal (0-1 km) temperature gradient map was generated using the SMU geothermal well database, which includes wells compiled by SMU (http://www.smu.edu/geothermal/), the USGS (Sass et al., 1999; http:/pubs.usgs.gov/of/1999/of99-425/webmaps/home.html; http://pubs.usgs.gov/of/2005/1207/), and other sources. Temperature gradients were derived in a multi-step process beginning with calculation of heat flow at individual wells, interpolation of heat flow between wells to produce a heat flow map (e.g., Blackwell and Richards, 2004), and then conversion of the heat flow map to a temperature gradient map using thermal conductivities assigned for grouped geological formations. Improvements in the spatial resolution of the gradient map for the Great Basin were obtained by assigning separate thermal conductivities to graben-filled Quaternary sediments, basement rocks in horst blocks, and regions of late Tertiary and Quaternary volcanic rocks. Purposely excluded from the initial calculations were known geothermal wells with heat flows >120 mW/m$^2$ and wells with isothermal or negative gradients. This was done so the predicted temperature gradients would not be overly influenced by geothermal systems.

**Seismicity Map (Figure 2D):** The seismicity map was generated by adding up all historical earthquake magnitudes within a 40 km radius of each grid cell in the model. The distance from the epicenter to the center of each cell was used to inversely weight individual earthquake magnitudes. To avoid a bias in the detection of earthquakes near seismograph stations, earthquakes were not included in the seismicity calculation unless they were strong enough to be detected anywhere in the Great Basin. Earthquakes with a magnitude of ≥4.8 were considered

strong enough to meet this criterion regardless of the year of occurrence, and Pancha et al. (in review) compiled these earthquakes from multiple catalogs. Due to improvements in the seismograph network that occurred around 1970, all earthquakes with a magnitude of 4.0 and greater that occurred during or after 1970 were considered detectable regardless of their epicenter location, and were added to this compilation. These lower-magnitude earthquakes came from two main catalog sources: the USGS National Earthquake Information Center and the Berkeley Advanced National Seismic System.

**Treatment of Regional Aquifers:** Most known high-temperature geothermal systems in the Great Basin (≥ 150°C) occur outside regional groundwater aquifers (Figure 3), including the Snake River Plain and Northwest Basalt aquifers in the northern Great Basin (USGS Principal Aquifers of the US; http://nationalatlas.gov/aquifersm.html) and the Carbonate aquifer in eastern Nevada and western Utah (Prudic et al., 1995). It is hypothesized that lateral groundwater flow could be capturing and entraining rising thermal fluids in these aquifers and suppressing the formation of hot springs and reducing near surface heat flow, thereby rendering those areas less completely explored than elsewhere in the Great Basin.

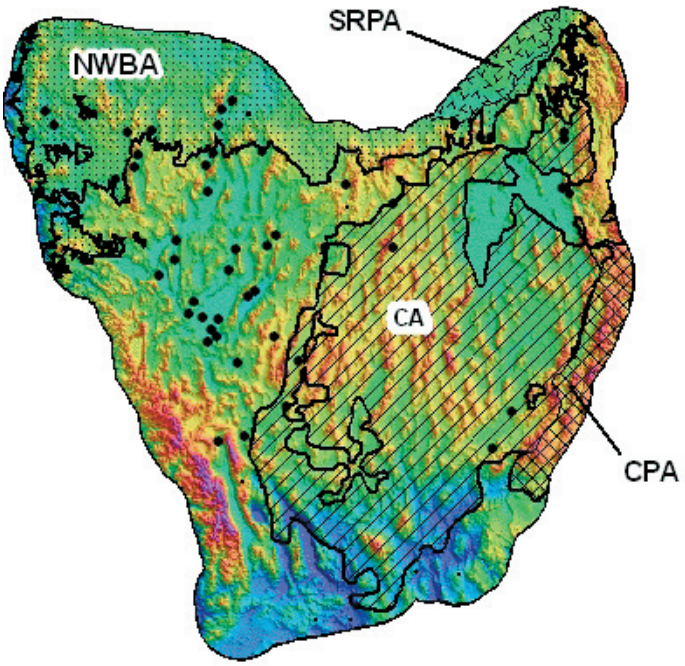


**Figure 3.** Regional aquifers in the Great Basin. Most known high temperature (≥ 150° C) geothermal systems lie outside areas underlain by the regional aquifers. Black circles are the extensional geothermal systems with temperatures ≥ 150° C that were used in the modeling exercise. CA = Carbonate aquifer; SRPA = Snake River Plains aquifer; NWBA = Northwest Basalt aquifer; CPA = Colorado Plateau aquifer. The background map is shaded topography.

In order to minimize potential bias with regard to aquifers in the favorability map, the geological and geophysical maps were pre-selected for their ability to model geothermal potential independent of the presence of those aquifers (at least at economic depths). As a first step, weights-of-evidence and logistic-regression model weights for each evidence map were calculated only in the non-aquifer areas (Figure 3). Those weights were then used to extrapolate geothermal favorability beneath areas having overlying regional aquifers. The logistic regression model accurately predicted 33 known geothermal training sites in non-aquifer regions, but predicted 23 training sites in the aquifer areas, whereas only 18 are known. This difference is statistically significant and suggests that the regional aquifers are either concealing geothermal systems or are underexplored relative to their non-aquifer counterparts.

## Magmatically-Heated Geothermal Systems

All known magmatically heated geothermal systems in the Great Basin are broadly restricted to the margins of the Great Basin and are closely associated with Quaternary silicic volcanic rocks (Koenig and McNitt, 1983). Consequently areas of the Great Basin with Quaternary silicic volcanic vents are very favorable for high temperature geothermal exploration. The locations of Quaternary silicic (rhyolite and rhyodacite) volcanic vents (Figure 1) were obtained from numerous sources, including the Great Basin Geoscience Database (Raines et al., 1996), and the Geothermal Resources of Utah CD (Blackett and Wakefield, 2002).

## Discussion

The ability of the geothermal map to correctly predict areas with good geothermal potential is dependent on many factors. One limitation involves the detail and accuracy of the digital data used to build the model. The historic earthquake record spans at best one hundred years, which is not enough to properly represent earthquake activities on some fault systems that may have recurrence intervals measured in thousands of years. Similarly, the number of bedrock-anchored GPS stations limits the resolution and accuracy of geodesy-based crustal strain estimates, and fault slip rate estimates are significantly constrained by the number of detailed trench studies. The acquisition of more gravity stations would sharpen the gravity/topographic map. Additionally, some types of geological information important for predicting geothermal activity have not been included in the model. For example, some rocks make better reservoir hosts than others. But because host rock lithologies at 1-4 km depths (the assumed range in production depth) are either unknown or are poorly constrained in many areas, host rock compositions were not used.

Another factor potentially limiting the map's predictive potential is the assumption that similar geologic processes control all extensional geothermal systems in the Great Basin. This is not likely to be entirely true, because regional differences in the tectonic setting, style of fracturing, fault-controlled permeability, and the composition of reservoir host rocks may exist across the Basin. In fact, some such differences are suggested when the geothermal system training sites are compared to each other with regards to their associated values from the input evidence maps. Geothermal systems within and adjacent to the Walker Lane, including geothermal systems in a northwest trend from Pyramid Lake, Nevada to Fallon, Nevada (Figure 1), have statistically significant lower values of

gravity/topographic gradients and higher values of earthquake sum/frequencies than do their geothermal system counterparts further to the east. This may be a reflection of a greater influence of strike-slip faulting in the Walker Lane, where pull-apart basins (e.g. Fish Lake Valley, Stockli, et al., 2003) and a transtensional environment may be more important in generating geothermal systems than they are in the central and eastern portion of the Basin, where normal extensional faulting may predominate. Future modeling research is planned to address some of these regional variations with the objective of building specialized models sensitive to subsets of extensional geothermal systems in the Great Basin.

In spite of the challenges involved with modeling, the predictive power of the map appears strong in many areas, including, for example, Dixie Valley, Surprise Valley, Railroad Valley, Summer Lake, Blue Mountain, New York Canyon, and the Gerlach area (Figure 1). Several of these areas did not have associated geothermal training sites used for modeling, so were not able to influence the results, but good favorability was predicted anyway. Highly favorable geothermal terrain is predicted for portions of the eastern and northeastern Great Basin near and north of Salt Lake City, and in the southwestern Great Basin in and beyond Death Valley—some of these areas may warrant a second look from exploration geologists. In any case, the map contains relatively detailed information and in many places provides a thought-provoking interpretation that stimulates curiosity.

## Acknowledgements

Publication of this map would not have been possible without the assistance of many individuals and organizations. Those not included under the list of authors include Don Sawatzky of the Arthur Brant Laboratory for Exploration Geophysics at UNR, who helped with customized GIS programming, Geoff Blewitt of the Nevada Geodetic Laboratory at the NBMG, Aasha Pancha of the Nevada Seismological Laboratory who provided comprehensive earthquake catalogs, Maria Richards at SMU, Catie Helm-Clark of the Idaho Engineering Laboratory, Gary Raines of the USGS who provided advice on spatial statistics, Tonya Boyd of the GeoHeat Center who provided state-by-state fluid geochemical files, and Tim Minor of the Desert Research Institute. Lisa Shevenell, current director, and Jane Long, former director of the GBCGE, provided key support and encouragement necessary to complete this project.

Funding for this research was made possible by a grant from the U.S. Department of Energy under instrument number DE-FG07-02ID14311. Gary Johnson and Elizabeth Crouse of the Nevada Bureau of Mines and Geology provided geographic information system (GIS) and cartographic services.

## References

Blackett, R.E. and Wakefield, S.I., 2002, Geothermal resources of Utah, a digital atlas of Utah's geothermal resources: Utah Geological Survey Open-File Report 397, CD-ROM.

Blackwell, D.D. and Richards, M., 2004, Geothermal Map of North America, AAPG, map item number 423, scale 1:6,500,000.

Boyd, T., 2002, Western states geothermal databases CD: Geothermal Resources Transactions, v. 26, p. 605-609.

Coolbaugh, M.F., 2003, The Prediction and Detection of Geothermal Systems at Regional and Local Scales in Nevada using a Geographic Information System, Spatial Statistics, and Thermal Infrared Imagery: Ph.D. dissertation, Reno, Nevada, University of Nevada, Reno, USA, 172 p.

Coolbaugh, M.F., Taranik, J.V., Raines, G.L., Shevenell, L.A., Sawatzky, D.L., Minor, T.B., and Bedell, R., 2002, A geothermal GIS for Nevada: defining regional controls and favorable exploration terrains for extensional geothermal systems: Geothermal Resources Council Transactions, v. 26, p. 485-490.

Coolbaugh, M., Zehner, R., Kreemer, C., Blackwell, D., Oppliger, G., Sawatzky, D., Blewitt, G., Pancha, A., Richards, M., Helm-Clark, C., Shevenell, L., Raines, G., Johnson, G., Minor, T., and Boyd, T., 2005, Preliminary geothermal map of the Great Basin, western United States: Nevada Bureau of Mines and Geology Map, under review (color jpg and pdf versions of the map can be obtained at http://www.unr.edu/geothermal/geothermal_gis2.htm).

Haines, A.J., and Holt, W.E., 1993, A procedure for obtaining the complete horizontal motions within zones of distributed deformation from the inversion of strain rate data: J. Geophys. Res., 98, 12057-12082.

Holt, W.E., Shen-Tu, B., Haines, J., and Jackson, J., 2000, On the determination of self-consistent strain rate fields within zones of distributed deformation, *in* Richards, M.A., Gordon, R.G., and van der Hilst, R.D., eds., The History and Dynamics of Global Plate Motions; p. 113-141, AGU, Washington, D.C.

Koenig, J.B. and McNitt, J.R., 1983, Controls on the location and intensity of magmatic and non-magmatic geothermal systems in the Basin and Range province: Geothermal Resources Council, Special Report No. 13, p. 93.

Kreemer, C., A.J. Haines, W.E. Holt, G. Blewitt, and D. Lavallée, 2000, On the determination of a global strain rate model, Earth Planets Space, 52, 765-770.

Machette, M.N., Haller, K.M., Dart, R.L., and Rhea, S.B., 2003, Quaternary fault and fold database of the United States: U.S. Geological Survey Open-File Report 03-417, http://qfaults.cr.usgs.gov/faults/.

Pancha, A., Anderson, J.G., and Kreemer, C., in review, Comparison of seismic, geodetic and geological scalar moment rates across the Basin and Range province: Bulletin of the Seismological Society of America.

Prudic, D.E., Harrill, J.R., and Burbey, T.J., 1995, Conceptual evaluation of regional groundwater flow in the carbonate-rock province of the Great Basin, Nevada, Utah, and adjacent states: U.S. Geological Survey Professional Paper 1409-D, 102 pp.

Raines, G.L., Sawatzky, D.L., and Connor, K.A., 1996, Great Basin Geoscience Data Base: USGS Digital Data Series DDS-041.

Sass, J.H., Priest, S.S., Blanton, A.J., Sackett, P.C., Welch, S.L., and Walters, M.A., 1999, Geothermal industry temperature profiles from the Great Basin: U.S. Geological Survey Open-File Report 99-425 (http://geopubs.wr.usgs.gov/open-file/of99-425/webmaps/home.html).

Stockli, D.F., Dumitru, T.A., McWilliams, M.O., and Farley, K.A., 2003, Cenozoic tectonic evolution of the White Mountains, California and Nevada: Geological Society of America Bulletin, v. 115, n. 7, p. 788-816.

Thelin, G. P., and Pike, R. J., 1991, Landforms of the conterminous United States - A digital shaded-relief portrayal: U. S. Geological Survey, Miscellaneous Investigation Series, Map 1-2206, scale 1: 350 000, Accompanying Booklet, 16 p.

Wisian, K.W., Blackwell, D.D. and Richards, M., 1999, Heat flow in the western United States and extensional geothermal systems: Proceedings 24th Workshop on Geothermal Reservoir Engineering, Stanford, CA, p. 219-226.

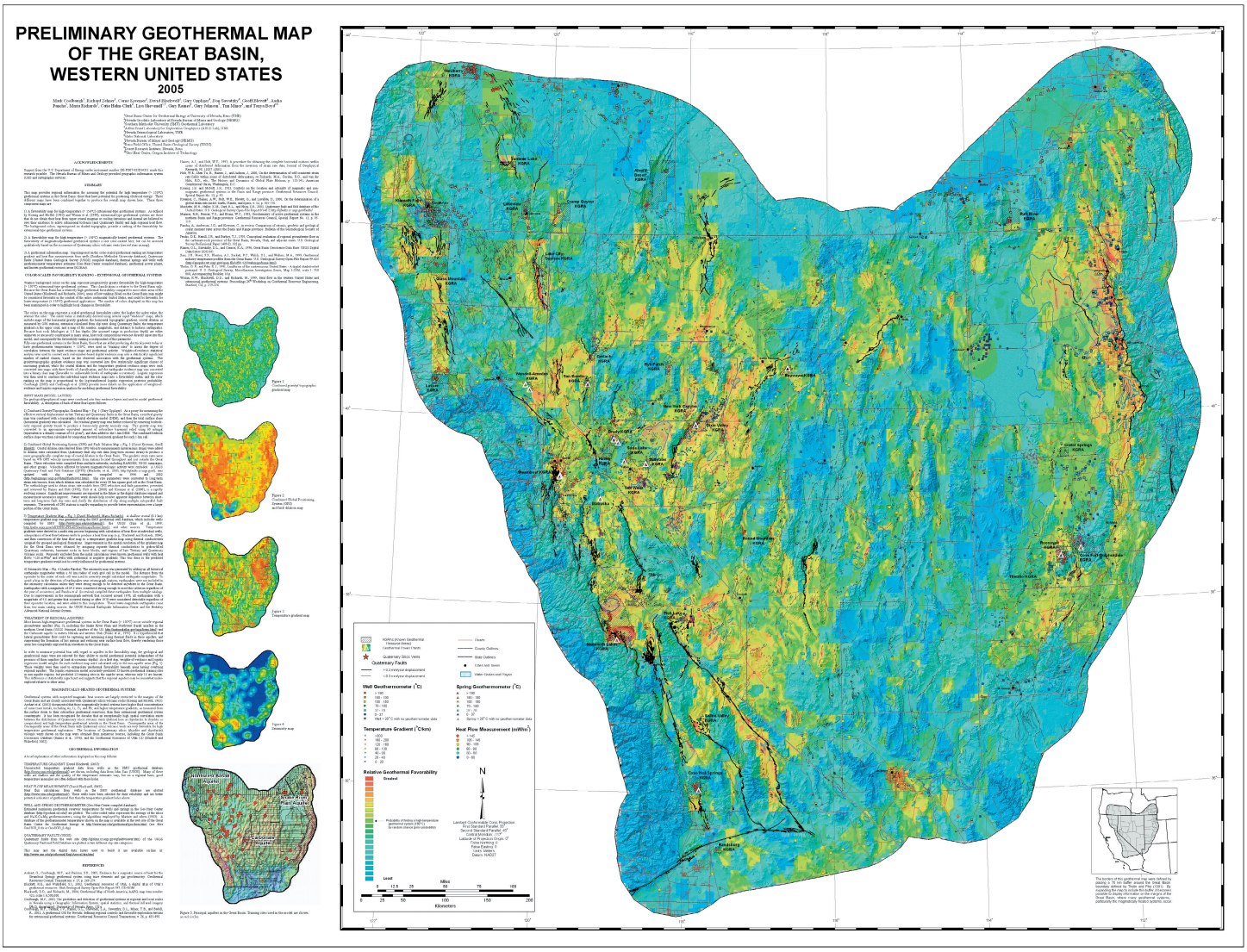


**Plate 1.** Prelimary Geothermal Map of the Great Basin, Western United States. The creation of this map is discussed in detail by Coolbaugh et al. (this volume), and this map represents Plate I for that paper. The final updated version of this map will be available before the end of 2005 in several formats at the web site of the Great Basin Center for Geothermal Energy at: http://www.unr.edu/geothermal/.